SCIENTIFIC REPORTS

OPEN

SUBJECT AREAS:
REPRODUCTIVE BIOLOGY
CELL DEATH

Received
20 October 2014

Accepted
22 December 2014

Published
26 January 2015

Correspondence and requests for materials should be addressed to S.L.K. (slk39@psu.edu)

ZnT2 is a critical mediator of lysosomal-mediated cell death during early mammary gland involution

Stephen R. Hennigar[1], Young Ah Seo[1], Supriya Sharma[1], David I. Soybel[1,2,3] & Shannon L. Kelleher[1,2,3,4]

[1]Department of Nutritional Sciences, The Pennsylvania State University, University Park, PA, USA, [2]Department of Surgery, Penn State Hershey College of Medicine, Hershey, PA, USA, [3]Department of and Cell and Molecular Physiology, Penn State Hershey College of Medicine, Hershey, PA, USA, [4]Department of Pharmacology, Penn State Hershey College of Medicine, Hershey, PA, USA.

Mammary gland involution is the most dramatic example of physiological cell death. It occurs through an initial phase of lysosomal-mediated cell death (LCD) followed by mitochondrial-mediated apoptosis. Zinc (Zn) activates both LCD and apoptosis *in vitro*. The Zn transporter ZnT2 imports Zn into vesicles and mitochondria and ZnT2-overexpression activates cell death in mammary epithelial cells (MECs). We tested the hypothesis that ZnT2-mediated Zn transport is critical for mammary gland involution in mice. Following weaning, ZnT2 abundance increased in lysosomes and mitochondria, which paralleled Zn accumulation in each of these organelles. Adenoviral expression of ZnT2 in lactating mouse mammary glands *in vivo* increased Zn in lysosomes and mitochondria and activated LCD and apoptosis, promoting a profound reduction in MECs and alveoli. Injection of TNFα, a potent activator of early involution, into the mammary gland fat pads of lactating mice increased ZnT2 and Zn in lysosomes and activated premature involution. Exposure of cultured MECs to TNFα redistributed ZnT2 to lysosomes and increased lysosomal Zn, which activated lysosomal swelling, cathepsin B release, and LCD. Our data implicate ZnT2 as a critical mediator of cell death during involution and importantly, that as an initial involution signal, TNFα redistributes ZnT2 to lysosomes to activate LCD.

Mammary gland involution is the most dramatic example of physiological cell death with about 80% of mammary epithelial cells (MECs) undergoing tightly regulated programmed cell death (PCD). Originally assumed to be an apoptosis-only event, recent studies reveal that PCD during mammary gland involution occurs through an initial phase of LCD (<24 h post-weaning)[1,2] followed by apoptosis thereafter[3–5]. LCD during involution is thought to occur through a multistep process where a stimulus initiates lysosomal membrane permeabilization (LMP), resulting in the upregulation and leakage of lysosomal contents such as cathepsins into the cytosol to act as executioner proteases[1,6]. To date, signal transducer and activator of transcription 3 (Stat3) has been implicated as a downstream regulator of LCD by upregulating expression of lysosomal cathepsins and suppressing expression of Spi2a, an endogenous inhibitor of cathepsins[1]; however, upstream signals that initiate LMP have yet to be identified. One possible signal is tumor necrosis factor alpha (TNFα), which is highly upregulated in the initial phase of involution and declines thereafter[7]. TNFα regulates leukemia inhibitory factor (LIF)[8], an upstream activator of Stat3[1,9], and importantly, induces LMP and LCD *in vitro*[6,10,11] and premature involution *in vivo*[8]. Although the precise mechanism is not well established, TNFα has been shown to induce lysosomal swelling[11] which may sensitize lysosomes to LMP, suggesting that TNFα may be an upstream regulator of LMP and LCD during the initial phase of mammary gland involution.

The initial phase of LCD may serve to maintain reversibility during episodic nursing; however, a second wave of PCD occurs >48 h post-weaning that facilitates irreversible remodeling of the mammary gland. The mechanism of PCD during the second irreversible phase of involution has not been identified, but is presumed to occur predominantly through mitochondrial-mediated apoptosis due to the withdrawal of systemic factors such as prolactin[4,5]. Contrary to cell death during early involution which is independent of executioner caspases[1], the intrinsic mitochondrial apoptotic pathway is activated by initiator caspases that cleave pro-apoptotic BH3 interacting-domain death agonist (Bid), into its truncated form (tBid), which is translocated to the mitochondria to initiate mitochondrial-mediated apoptosis. The mechanisms through which specific local factors activate PCD and involution are not understood.

Zinc (Zn) is known to modulate PCD *in vitro*. Zn accumulation in lysosomes is implicated as an activator of LCD in neurons[12,13] and breast cancer cells[14]. In addition, mitochondrial Zn accumulation activates mitochondrial-mediated apoptosis[15] through the release of cytochrome *c* followed by caspase activation[16,17]. The Zn transporter ZnT2 (*SLC30A2*) is a six transmembrane protein with N- and C-termini within the cytoplasm that is found exclusively in highly specialized secretory tissues, such as the prostate and mammary gland[18,19]. Interestingly, ZnT2 drives Zn accumulation into vesicles[18] and mitochondria[20] in MECs which decreases ATP production and mitochondrial oxidation and increases apoptosis *in vitro*[20]. However, a role for ZnT2 in PCD during mammary gland involution has not been shown.

Herein, we found that ZnT2 plays a critical and multifactorial role in PCD leading to mammary gland involution. ZnT2 drives Zn into lysosomes to activate LCD and mitochondria to activate apoptotic cell death. Adenoviral expression of ZnT2 in mammary glands of lactating mice *in vivo* activated LCD and apoptosis and initiated premature involution. Moreover, using *in vivo* and *in vitro* models we found that as an initial involution signal, TNFα regulated ZnT2-mediated Zn redistribution to lysosomes and specifically, activated LCD and attenuation of ZnT2 eliminated the response to TNFα. Taken together our work provides compelling evidence that ZnT2-mediated Zn transport is a critical regulatory component of mammary gland involution.

Results

ZnT2 accumulates Zn in lysosomes and mitochondria during mammary gland involution. We previously reported that the mammary gland accumulates Zn during lactation[21]. Herein, we found that similar to calcium[22], Zn accumulation in the mammary gland was further augmented during involution (Fig. 1a). To determine where Zn accumulated, we isolated subcellular fractions enriched in specific organelles using density fractionation. Organelle enrichment was confirmed by immunoblotting for specific organelle markers for mitochondria, lysosomes, and the endoplasmic reticulum/Golgi apparatus (Supplementary Fig. S1a). We found that the Zn concentration in lysosome-enriched fractions isolated from involuting mammary glands was significantly higher than identical fractions isolated from lactating mammary glands (Fig. 1b). Moreover, we noted that the abundance of ZnT2 in lysosome-enriched fractions was higher during the initial phase of involution (24 h post weaning) (Fig. 1c). Acid phosphatase (EC 3.1.3.2) is a lysosomal enzyme that requires Zn to hydrolyze the substrate, nitrophenyl phosphate[23]. Consistent with previous reports noting that acid phosphatase activity is highest during early involution and declines 48 h post-weaning[24], we found that peak ZnT2 abundance in lysosomes corresponded with peak acid phosphatase activity (Supplementary Fig. S1b). Concurrently, Figure 1d shows that the Zn concentration of mitochondria increased as involution progressed which paralleled an increase in mitochondrial ZnT2 abundance (Fig. 1e). Although the abundance of ZnT2 in specific fractions was altered, this was not a consequence of changes in the total abundance of ZnT2 (Supplementary Fig. S2a). Taken together, these data suggest that ZnT2 expression is associated with Zn accumulation in lysosomes and mitochondria during the early stages of mammary gland involution.

Forced adenoviral expression of ZnT2 activates premature involution. To determine if ZnT2-mediated Zn accumulation in lysosomes and mitochondria activates PCD and premature involution *in vivo*, we used an adenovirus vector to drive ZnT2-mediated Zn accumulation into both organelles in lactating mice. Adenovirus vectors are a proven method to successfully transduce MECs from parturition to >5 days of lactation without inducing inflammation *in vivo*[25]. We created an adenoviral vector expressing HA-tagged ZnT2 (AdZnT2) or β-galactosidase (AdLacZ; control vector) and AdZnT2 localization and function was confirmed in cultured MECs (Supplementary Fig. S3). We gently infused AdZnT2 and AdLacZ intraductally into mammary glands 4 and 5 or 9 and 10, respectively, of late pregnant (gestation day 17) mice (Supplementary Fig. S4a) allowing each mouse to serve as its own control. Virus infusion into the primary duct of the mammary gland cannot be achieved after the onset of lactation due to the presence of milk in the ducts as reported previously[26]. Dams were allowed to deliver naturally and nurse their offspring for 2–3 days. There was no indication that AdLacZ-infused mammary glands (9/10) were preferentially suckled (i.e. all nipples were swollen and pink and milk was expelled from all nipples when gently squeezed). Immunohistochemical analysis of mammary glands using anti-HA antibody confirmed the efficient transduction of AdZnT2 *in vivo* (Fig. 2h and Supplementary Fig. S4b). We found that mammary glands expressing the ZnT2 adenovirus accumulated ~32% more Zn ($P < 0.05$) compared with mammary glands transduced to express β-galactosidase as a control (Fig. 2a). AdZnT2-expressing mammary glands accumulated 30% more Zn ($P < 0.001$) in lysosome-enriched fractions (Fig. 2b), which was associated with a 25% increase ($P < 0.001$) in acid phosphatase activity (Supplementary Fig. S4c). Increased lysosomal Zn corresponded to LMP and LCD, as noted by cathepsin B immunofluorescent staining (Fig. 2e), an ~2-fold increase ($P < 0.001$) in cytosolic cathepsin B activity (Fig. 2f), and pStat3 immunofluorescent staining (Fig. 2h) in AdZnT2-expressing mammary glands. Mitochondrial Zn concentration was also greater in AdZnT2-expressing mammary glands (Fig. 2c) and we observed a significant two-fold increase ($P < 0.001$) in the percentage of TUNEL-positive cells (Fig. 2d) in mammary glands expressing the ZnT2 adenovirus compared with mammary glands transduced with the control vector. We next examined mammary gland architecture using whole mount analysis (Fig. 2g). The architecture of mammary glands from mice infused with the control virus resembled that of normal mammary glands during lactation[27], confirming that the transduction and over-expression of a protein in the lactating mammary gland did not itself activate involution. In contrast, the architecture of mammary glands from mice expressing the ZnT2 adenovirus had disintegrated acini and displayed characteristic morphological features of involution[27]. Involution was confirmed by detection of pStat3 immunofluorescence in AdZnT2-expressing mammary glands but not in AdLaZ-expressing controls (Fig. 2h). Collectively, this indicates that ZnT2-mediated Zn accumulation is a critical factor in activating the early stage of PCD at the onset of mammary gland involution.

Injection of TNFα into lactating mammary glands accumulates Zn in lysosomes. The gene expression profile of TNFα shows that TNFα is highly upregulated in the initial phase of involution and declines thereafter[7]. Although TNFα induces LMP and LCD *in vitro*[6,10,11] and initiates premature involution *in vivo*[8] the mechanisms through which TNFα exerts these effects are not well understood. We tested the hypothesis that as an induction signal, TNFα redistributes ZnT2-mediated Zn accumulation into lysosomes to activate the initial phase of mammary gland involution. We first gently injected TNFα or saline into mammary gland fat pads 4 and 9, respectively, of lactating mice (lactation day 7–10). Offspring were returned to the dams and offspring suckling was observed. The mammary glands were dissected 24 h after TNFα injection and H&E staining confirmed that TNFα induced involution (Supplementary Fig. S5) as previously described[8]. Mammary glands injected with TNFα accumulated 30% more Zn ($P < 0.05$) than mammary glands injected with saline (Fig. 3a). The Zn concentration of lysosome-enriched fractions was higher in TNFα-injected mammary glands ($P < 0.001$) compared with saline-injected controls (Fig. 3b). Importantly, injection of TNFα increased the abundance of ZnT2 in lysosome-enriched fractions (Fig. 3d). Moreover, cathepsin B

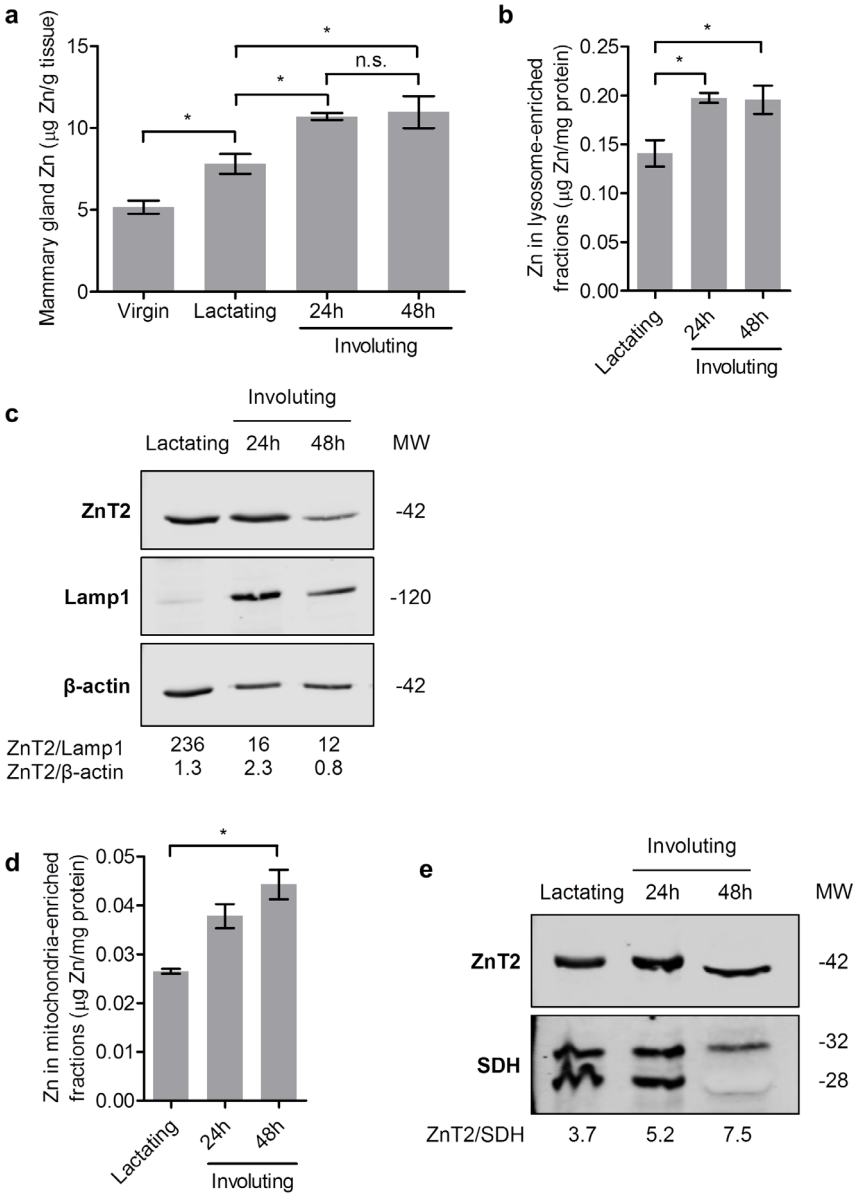

Figure 1 | ZnT2 accumulates Zn in lysosomes and mitochondria in mouse mammary glands during involution. (a) Mammary glands (~0.1–0.2 g) from virgin, lactating, and 24- and 48 h involuting mice were digested in nitric acid and Zn concentration was measured by atomic absorption spectroscopy. Data represent mean μg Zn/g tissue ± SD; $n = 5$/group, $^*P < 0.05$, n.s., not significant. (b)–(e) Lysosome- and mitochondria-enriched fractions were isolated from lactating and 24- and 48 h involuting mammary glands by differential centrifugation. (b) Lysosomal Zn concentration from lactating and involuting mammary glands. Fractions were digested in nitric acid and concentration was measured by atomic absorption spectroscopy. Data represent mean μg Zn/mg protein ± SD; $n = 4$/group, $^*P < 0.05$. (c) Representative immunoblot of ZnT2 and Lamp1 (lysosomal marker) in lysosome-enriched fractions isolated from lactating and involuting mammary glands. β-actin was used as a loading control and ratios of signal intensities are reported under the blot. (d) Isolated mitochondria-enriched fractions from lactating and involuting mammary glands were digested in nitric acid and Zn concentration was measured by atomic absorption spectroscopy. Data represent mean μg Zn/mg protein ± SD; $n = 3$/group, $^*P < 0.05$. (e) Protein abundance of ZnT2 in mitochondria-enriched fractions isolated from lactating and involuting mammary glands was determined by immunoblot and expressed relative to the mitochondrial marker succinate dehydrogenase (SDH). Ratios of signal intensities are reported under the blot.

immunofluorescent staining was detected in TNFα-injected mammary glands but not in saline-injected controls (Fig. 3f), which corresponded to a significant increase ($P < 0.001$) in cathepsin B activity in cytosolic fractions (Fig. 3g) and immunofluorescent staining of pStat3 (Fig. 3h) in TNFα-injected mammary glands compared to saline-injected controls. The Zn concentration of mitochondria–enriched fractions showed a small increase that was not statistically significant (Fig. 3c) and we failed to detect ZnT2 in mitochondria-enriched fractions of TNFα-injected mammary glands (Fig. 3e). This suggests that TNFα regulates ZnT2-mediated Zn accumulation in lysosomes during the initial phase of involution to activate LCD.

TNFα mediates the redistribution of ZnT2 to lysosomes to activate LCD in cultured MECs. Based on our findings that injection of TNFα into the lactating mammary gland was associated with ZnT2-mediated Zn accumulation in lysosomes *in vivo*, we tested the hypothesis that the effects of TNFα *in vivo* were mediated through direct effects on LCD in MECs. MECs treated with TNFα retained ~40% more Zn compared with untreated cells (Fig. 4a). Zn uptake was unaffected (Fig. 4b). We next used FluoZin-3-AM as a reporter of labile Zn pools[28] to determine where Zn accumulated in response to TNFα. Using confocal microscopy, we found that FluoZin-3-AM fluorescence colocalized with LysoTracker Red

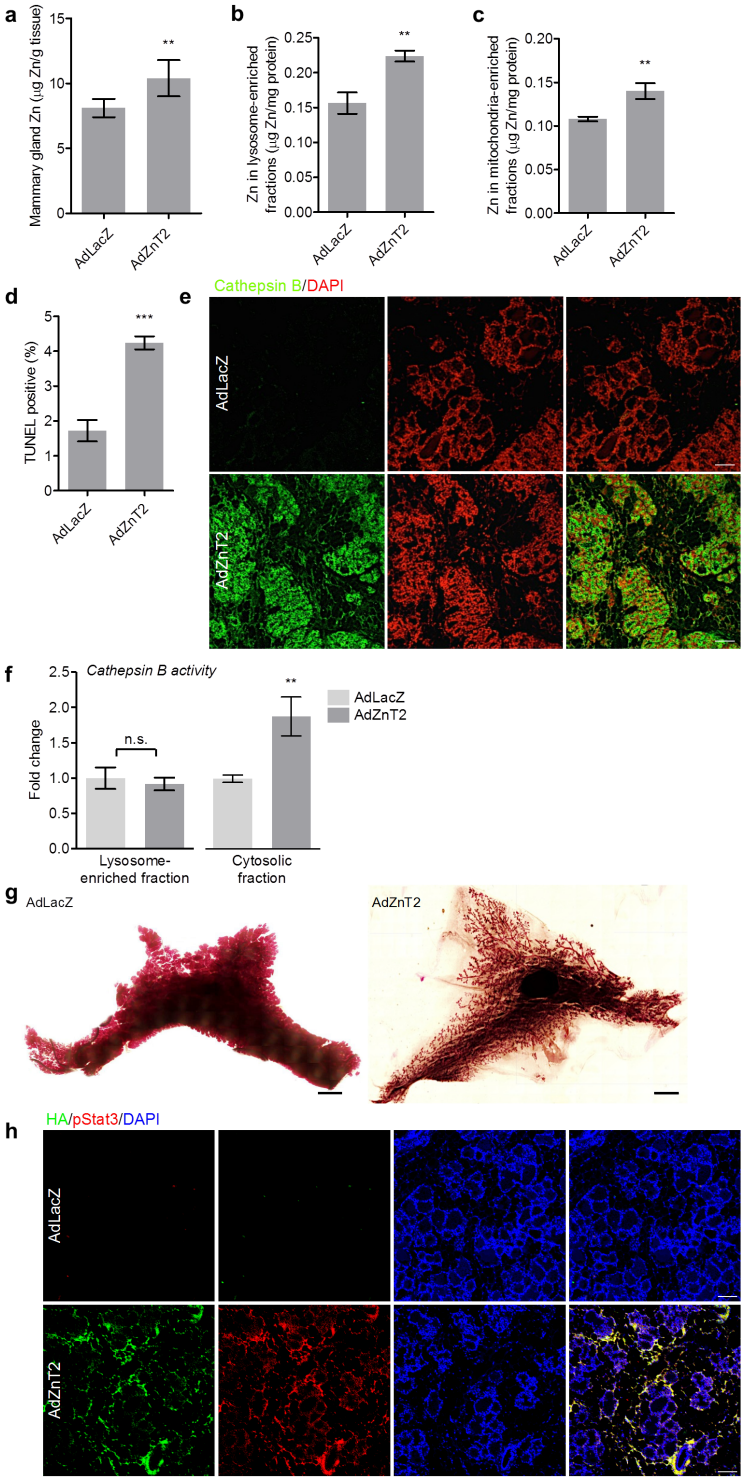

Figure 2 | Adenoviral expression of ZnT2 increases LCD and apoptosis and initiates premature involution. (a) Mammary glands from AdLacZ and AdZnT2 mice were digested in nitric acid and Zn concentration was measured by atomic absorption spectroscopy. Data represent mean μg Zn/g tissue ± SD; $n = 9$/group, $^{**}P < 0.001$. (b)–(c) Zn concentration of lysosome- and mitochondria-enriched fractions isolated from AdLacZ- and AdZnT2-expressing mammary glands. Fractions were digested in nitric acid and concentration was measured by atomic absorption spectroscopy. Data represent mean μg Zn/mg protein ± SD; $n = 4$/group, $^{**}P < 0.001$ and $^{***}P < 0.0001$. (d) TUNEL staining in AdZnT2-transduced mammary glands and compared with mammary glands transduced with AdLacZ. Data represent percentage of TUNEL positive staining cells ± SD; $n = 5$ mice/group, $^{***}P < 0.0001$. (e) Immunofluorescent staining of cathepsin B and DAPI in AdLacZ- and AdZnT2-expressing mammary glands. Scale bars = 100 μm. (f) Cathepsin B activity in lysosome-enriched and cytosolic fractions isolated from mammary glands of AdLacZ and AdZnT2 mice. Data represent fold increase in activity ± SD; $n = 4$ mice/group, $^{**}P < 0.001$. (g) Whole mounts from mammary glands transduced with AdLacZ (top) showed normal mammary gland morphology with expanded alveoli during lactation. In contrast, mammary glands expressing the ZnT2 adenovirus (AdZnT2, bottom) had disintegrated acini in which the terminal end buds were considerably regressed. Scale bar = 2 mm. (h) Immunofluorescent staining of HA and pStat3 from mammary glands transduced with AdLacZ or AdZnT2. HA fluorescence was only detected in sections from mammary glands transduced with AdZnT2-HA, which also expressed pStat3. Scale bars = 100 μm.

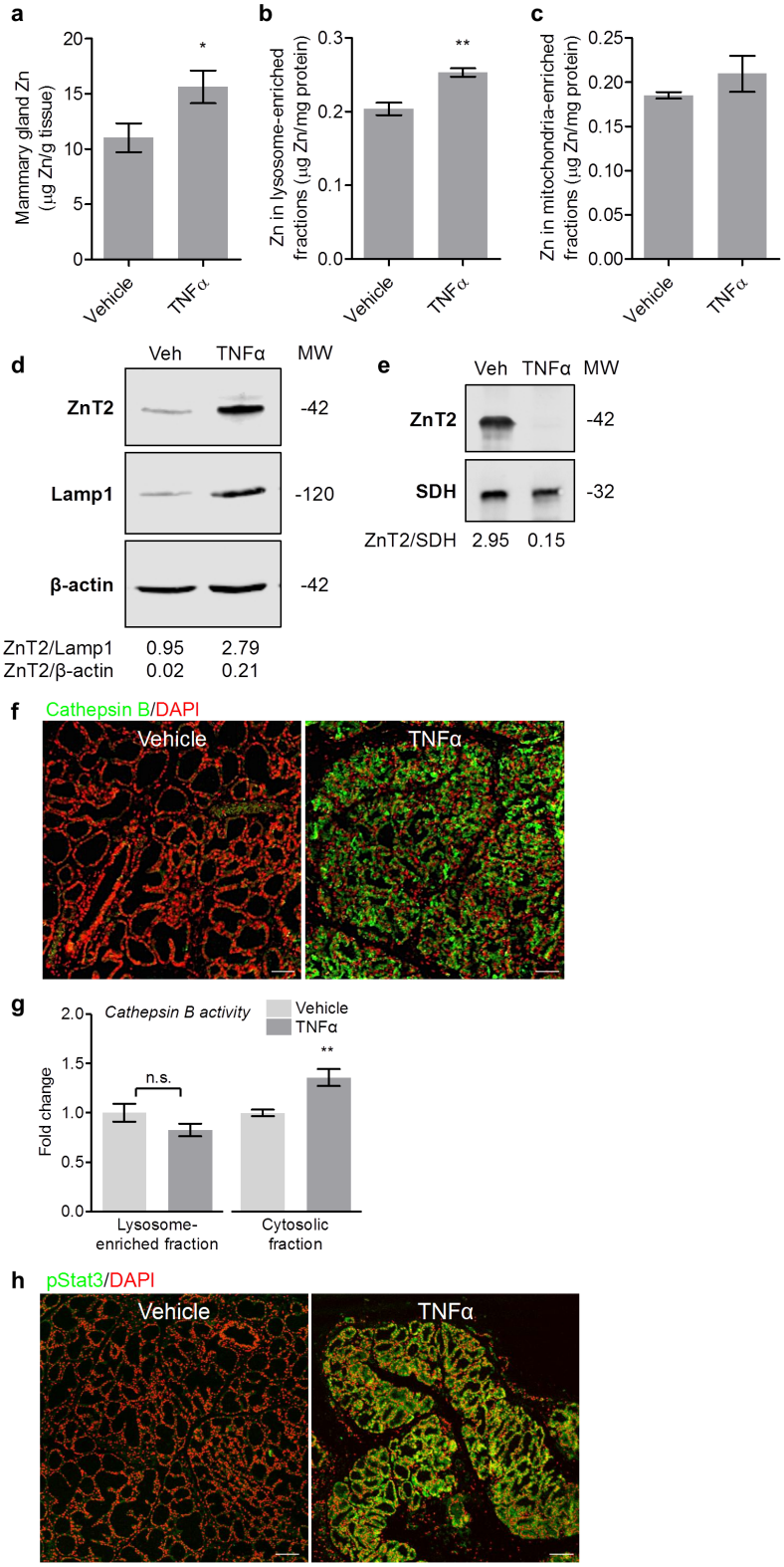

Figure 3 | TNFα accumulates Zn in lysosomes *in vivo*. TNFα (1 μg) or saline vehicle was injected into the mammary glands of lactating mice and mammary glands were collected 24 h post-injection. (a) Mammary glands from TNFα and vehicle injected mice were digested in nitric acid and Zn concentration was measured by atomic absorption spectroscopy. Data represent mean μg Zn/g tissue ± SD; $n = 5$/group, $^{*}P < 0.05$. (b)–(c) Zn concentration of lysosome- and mitochondria-enriched fractions isolated from vehicle- and TNFα-injected mammary glands. Fractions were digested in nitric acid and concentration was measured by atomic absorption spectroscopy. Data represent mean μg Zn/mg protein ± SD; $n = 5$/group, $^{**}P < 0.001$. (d)–(e) Protein abundance of ZnT2 in lysosome- and mitochondria-enriched fractions isolated from vehicle- (Veh) and TNFα-injected mammary glands was determined by immunoblot. Lamp1 was used to verify the presence of lysosomes and β-actin and SDH were used as loading controls. Ratios of signal intensities are reported under the blots. (f) Immunofluorescent staining of cathepsin B and DAPI in vehicle- and TNFα-injected mammary glands. Scale bars = 100 μm. (g) Cathepsin B activity in lysosome-enriched and cytosolic fractions isolated from vehicle- and TNFα-injected mammary glands. Data represent fold increase in activity ± SD; $n = 4$ mice/group, $^{**}P < 0.001$.

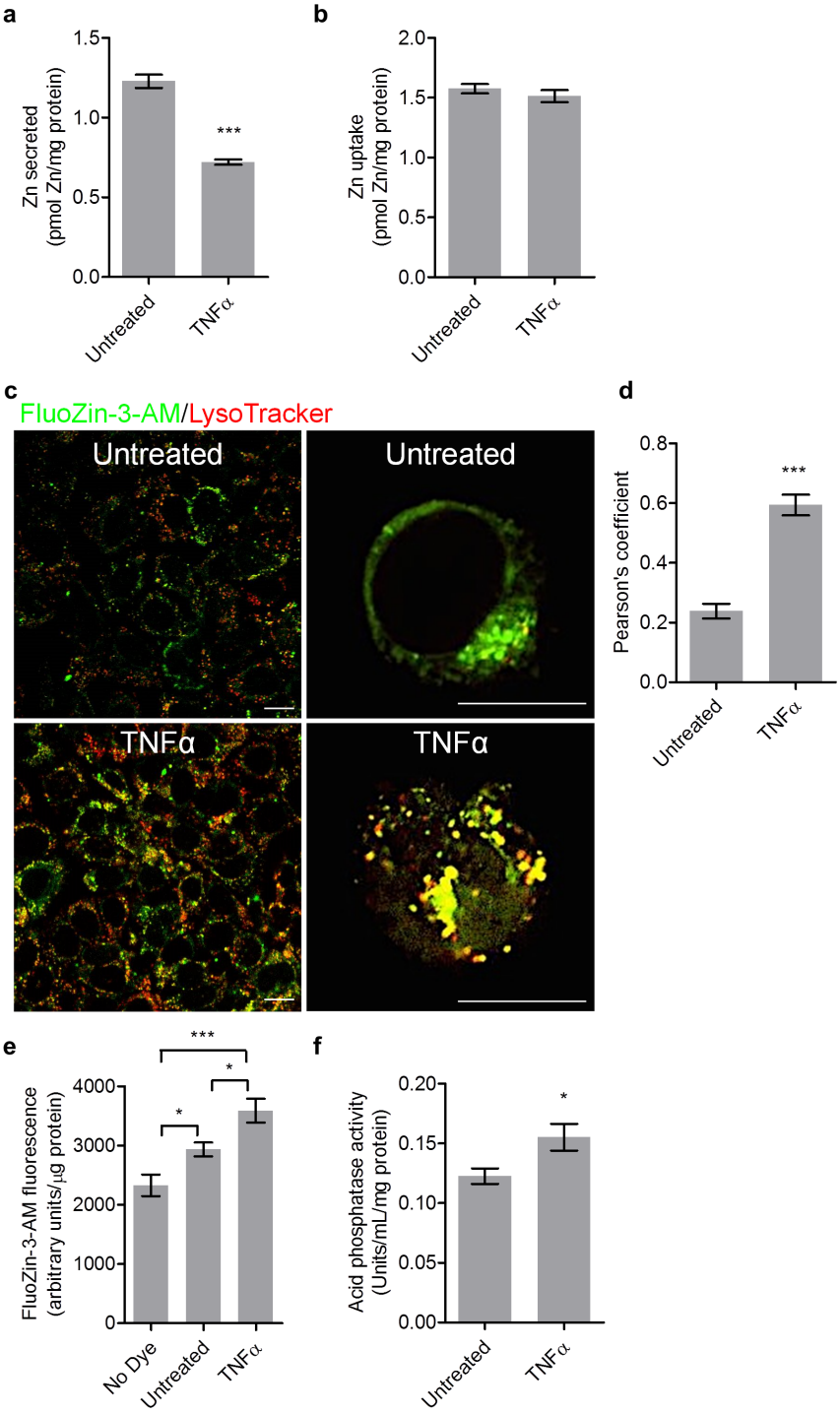

Figure 4 | TNFα accumulates Zn in MECs *in vitro*. ^{65}Zn-labeled cells were treated with TNFα or left untreated and Zn secretion (a) and Zn uptake (b) were quantified in conditioned media and cells, respectively, using a γ-scintillation counter. Values represent mean pmol Zn/μg protein ± SD; $n = 12$ samples/treatment, $^{***}P < 0.0001$. (c) Representative live cell images of intracellular Zn pools in untreated and TNFα-treated cells. FluoZin-3-AM, an indicator of labile Zn pools (green), colocalized (merge, yellow) with the lysosomal marker, LysoTracker Red in cells treated with TNFα. Cells are viewed at 60 × (left panels) or 100 × magnification (right panels). Scale bars = 10 μm. (d) Pearson's correlation coefficient for colocalization of FluoZin-3-AM (Zn, green) and LysoTracker (lysosomes, red). Data represent mean ± SD of at least 5 fields of view from three independent experiments. $^{***}P < 0.0001$. (e) Labile Zn pools were quantified using FluoZin-3-AM in cells treated with TNFα and compared to untreated cells. Cells with no FluoZin-3-AM (No dye) are included to account for background fluorescence. Values represent mean fluorescence/μg protein ± SD, $n = 8$/treatment. Experiment was conducted three independent times. $^{*}P < 0.05$ and $^{***}P < 0.0001$. (f) Acid phosphatase activity in untreated and TNFα-treated cells. Data represent mean acid phosphatase activity (Units/mL/mg protein) ± SD, $n = 8$/treatment. Experiment was conducted three independent times. $^{*}P < 0.05$.

(Fig. 4c), which was reflected in a 60% increase in the Pearson's coefficient (Fig. 4d). Importantly, cells treated with TNFα had significantly higher (22%, $P < 0.05$) FluoZin-3-AM fluorescence (Fig. 4e) coinciding with a significant increase (27%, $P < 0.05$) in acid phosphatase activity (Fig. 4f) confirming that TNFα stimulates Zn accumulation in lysosomes. We previously showed that ZnT2 is not localized to lysosomes in MECs under basal conditions[18,21]; however, in response to TNFα, ZnT2 colocalized with the lysosome

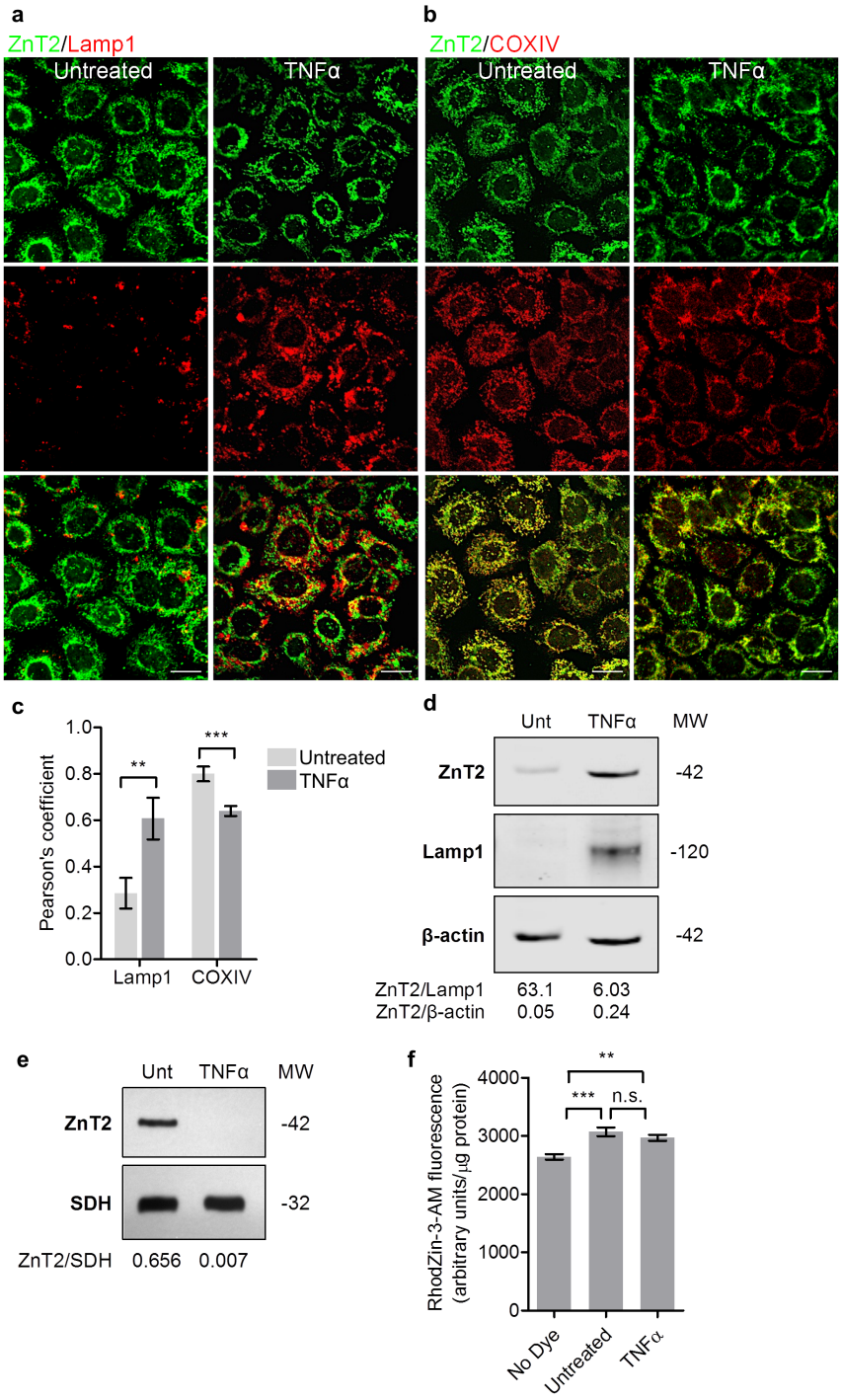

Figure 5 | TNFα redistributes ZnT2 away from the secretory compartment and mitochondria to lysosomes. Representative confocal images showing ZnT2 (green) colocalized (merge, yellow) with (a) Lamp1 (red, lysosomal marker) in TNFα-treated cells. ZnT2 was not localized to lysosomes in untreated cells. ZnT2 (green) colocalized (merge, yellow) with (b) COX IV (red, mitochondrial marker) in untreated cells. ZnT2 was not localized to mitochondria in TNFα-treated cells. Scale bars = 10 μm. (c) Pearson's correlation coefficient for colocalization of endogenous ZnT2 (green) and Lamp1 or COXIV (red). Data represent mean ± SD of at least 5 fields of view from three independent experiments. $^{**}P < 0.001$ and $^{***}P < 0.0001$. (d)–(e) Protein abundance of ZnT2 in lysosome- and mitochondria-enriched fractions from untreated (Unt) and TNFα-treated cells was determined by immunoblot. Lamp1 was used to verify the presence of lysosomes and β-actin and SDH were used as loading controls. Ratios of signal intensities are reported under the blots. (f) Mitochondrial Zn pools were quantified using RhodZin-3-AM in cells treated with TNFα and compared to untreated cells. Cells with no RhodZin-3-AM (No dye) are included to account for background fluorescence. Values represent mean fluorescence/μg protein ± SD, $n = 8$/treatment. Experiment was conducted three independent times. $^{**}P < 0.001$, $^{***}P < 0.0001$ and n.s., not significant.

marker Lamp1 (Fig. 5a and c) and increased in abundance in lysosome-enriched fractions (Fig. 5d). TNFα did not affect the total amount of ZnT2 (Supplementary Fig. S6) indicating that TNFα regulates ZnT2 in a post-translational manner to redistribute ZnT2 to lysosomes. Interestingly, we did not detect ZnT2 in mitochondria (Fig. 5b and e) in TNFα-treated cells and mitochondrial Zn pools (assessed by RhodZin-3-AM fluorescence[29]) remained unchanged (Fig. 5f).

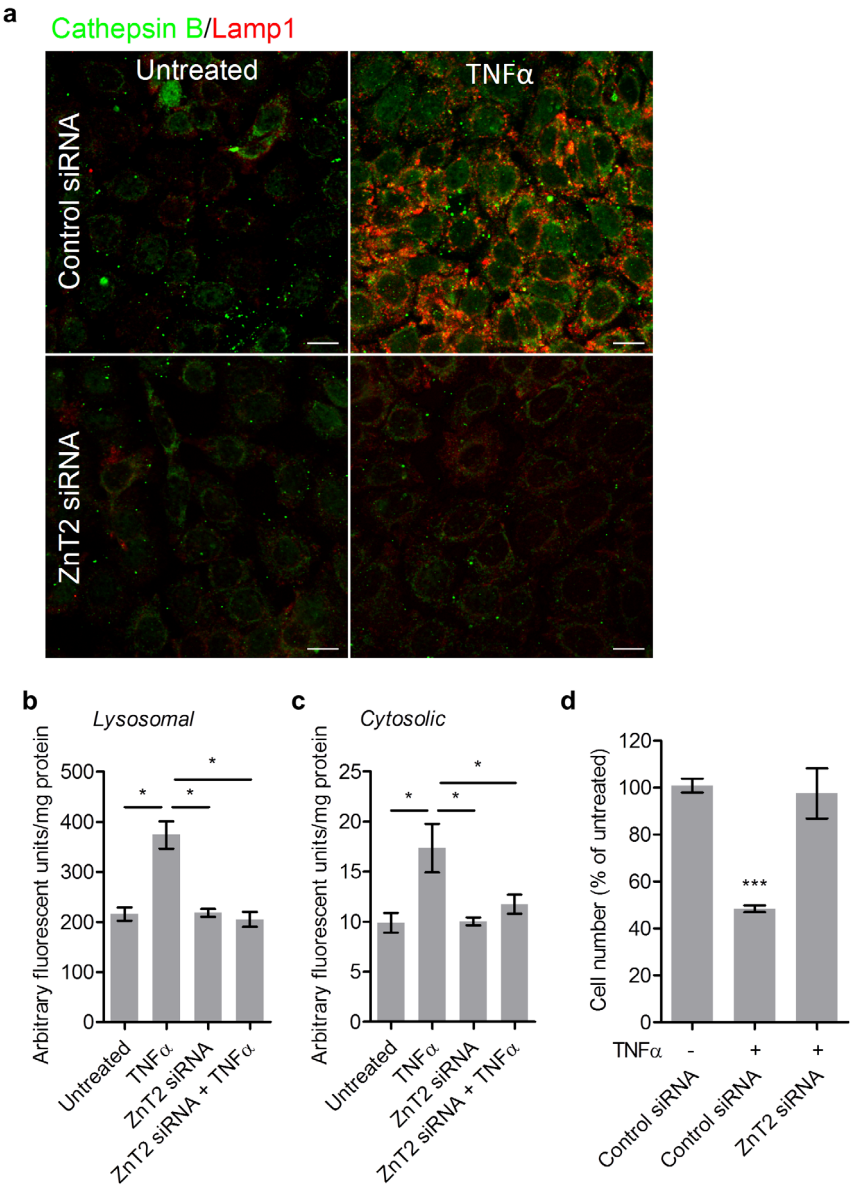

Figure 6 | Expansion of lysosomal Zn pools via ZnT2 increases LCD. (a) Co-immunofluorescence of Lamp1 and cathepsin B demonstrating that TNFα augmented the presence of lysosomes and cytosolic cathepsin B compared to control siRNA transfected cells and that ZnT2 attenuation abrogated this effect. Scale bars = 10 μm. (b)–(c) Increased cathepsin B activity in lysosome-enriched and cytosolic fractions isolated from TNFα stimulated compared to control siRNA transfected and ZnT2 attenuated cells. The data are the fold change ± SD of three independent experiments; $n = 3$/treatment, $^{*}P < 0.05$. (d) Cell number decreased in response to TNFα and ZnT2 attenuation rescued this effect. Data represent cell number as a percentage of control siRNA transfected cells ± SD, $n = 3$/treatment. Experiment was conducted three independent times. $^{***}P < 0.0001$. For all experiments cells were treated with ZnT2 siRNA or control siRNA followed by ± TNFα (15 ng/mL) for 24 h.

To confirm that ZnT2-mediated lysosomal Zn accumulation resulted in functional consequences, we examined hallmarks of LCD. Co-immunofluorescent staining of Lamp1 and cathepsin B showed that TNFα augmented the number of lysosomes and cathepsin B release (Fig. 6a). Importantly, ZnT2 attenuation (Supplementary Fig. S7) eliminated the effect of TNFα on lysosome size and/or number and cathepsin B release. These findings corresponded to a significant increase ($P < 0.05$) in cathepsin B activity in lysosome-enriched fractions (Fig. 6b) and cytosolic fractions ($P < 0.05$; Fig. 6c) isolated from cells treated with TNFα compared to identical fractions isolated from control siRNA transfected and ZnT2 attenuated cells. Finally, TNFα stimulation activated cell death and lead to a 50% reduction in cell number compared to untreated cells (Fig. 6d). Importantly, using cells in which we attenuated ZnT2 expression we found that TNFα only activated cell death in the presence of ZnT2. Collectively, this indicates that TNFα-induced activation of LCD in MECs is dependent upon ZnT2-mediated Zn transport.

Discussion

Mammary gland involution is a well-orchestrated series of PCD events that occur in a tightly regulated, time-dependent fashion[3]. Recent work indicates that the initial phase of involution is driven by LCD[1,2], which mediates dead cell clearance and suppresses inflammation[30]. Subsequently, mitochondrial-mediated apoptosis is thought to facilitate the irreversible remodeling of the mammary gland to the pre-pregnant state. Zn stimulates both LCD[12–14] and apoptosis[15] *in vitro*. In this study, we demonstrated that ZnT2-mediated Zn redistribution is a critical regulatory component of early involution mechanisms. We propose that ZnT2 is a critical

mediator of cell death during early involution by accumulating Zn into lysosomes to activate LCD and mitochondria to activate mitochondrial-mediated apoptosis. Importantly, we identified TNFα as a critical regulatory factor in the initial activation of involution.

Watson and colleague's recent identification of the lysosomal-mediated pathway as the primary mode of PCD during the initial phase of mammary gland involution[1] was the first to describe this cell death mechanism under physiological conditions. This multi-step pathway is initiated by a stimulus that induces LMP and is followed by the execution of PCD by lysosomal enzymes released into the cytosol. Although Stat3 has been shown to contribute to the downstream execution of LCD during involution[1], upstream signals that initiate LMP have yet to be identified. Because TNFα induces LMP[6,10,11] and acts during the initial phase of involution[7,8], we proposed a role for TNFα as an initial activator of LCD during mammary gland involution. A key finding from our study is that TNFα post-transcriptionally regulates the redistribution of ZnT2 to lysosomes, identifying a novel role for TNFα as a critical upstream initiator of LMP and LCD during early involution. An alternative possibility is that there are simply more lysosomes during involution. One important consequence of lysosomal Zn accumulation may be to increase the activity of Zn-dependent enzymes within the lysosome, such as acid phosphatase[24,31] and acid-sphingomyelinase[32], increasing the susceptibility for LMP. In addition, Zn-induced oxidative stress may increase aldehyde by-products of lipid peroxidation[12], causing the disruption of lysosomal membranes and activation of LMP. Intriguingly, we noted that TNFα could not stimulate the observed increase in lysosome size and/or number in ZnT2-attenuated cells. This suggests that ZnT2-mediated Zn transport may be coupled to the generation of a proton gradient[33] and necessary for lysosome biogenesis. Alternatively, intraluminal Zn binds negatively charged head groups of fatty acids, such as lysobisphosphatidic acid (LBPA) in the internal membranes of late endosomes and lysosomes[34] which is critical for lysosome biogenesis[35]. However, it may not be intraluminal Zn accumulation, but the clearance of Zn from the cytosol that is important for the expansion of the lysosomal compartment and LCD. For example, depletion of cytosolic Zn may activate lysosome biogenesis by repressing mTOR (mechanistic target of rapamycin)[36], thereby allowing the dephosphorylation and subsequent translocation of Transcription Factor EB (TFEB) to the nucleus to induce the CLEAR (Coordinated Lysosomal Expression and Regulation) gene network[37]. Genes belonging to the CLEAR network all contain a palindromic 10-base pair GTCACGTGAC motif in their promoter that overlaps the E-box that TFEB binds to activate transcription of genes important for lysosome biogenesis and function[38]. Thus, failure to incorporate Zn into lysosomes and activate the CLEAR network may impair lysosome biogenesis.

It is particularly interesting that TNFα redistributed ZnT2 to lysosomes, as ZnT2 is not normally found in lysosomes nor does Zn accumulate in lysosomes in MECs under basal conditions or in response to lactogenic stimuli[18,21]. Emerging evidence suggests that the localization and function of an increasing number of Zn transporters are modified post-translationally, providing a rapid and importantly, reversible, regulatory response. For example, treatment of cells with exogenous Zn, post-translationally redistributes the ZnT2 homolog, ZnT4, from the Golgi apparatus to the cell membrane for Zn efflux from the mammary epithelial cell[39]. Another ZnT2 homolog, ZnT3, is also post-translationally trafficked to synaptic-like microvesicles by tyrosine dimerization[40]. Lysosomal proteins contain specific sorting signals such as dileucine-based motifs (DXXLL or [DE]XXXL[LI]) or tyrosine-based motifs (YXXØ; where X = any residue, Ø = large hydrophobic residues)[41] in the cytoplasmic domains, which interact with components of clathrin coats or adaptor protein (AP) complexes[41]. Examination of the amino acid sequence of ZnT2 reveals the presence of two conserved dileucine motifs (Leu^{9} in the N-terminus and Leu^{293} in the C-terminus). Precedence for targeted redistribution of ZnTs exists as a motif in the C-terminal tail of ZnT3[42] interacts with AP-3 to preferentially target ZnT3 to distinct acidophilic synaptic vesicles[43]. Examination of the primary sequence of the C-terminal tail of ZnT3 notes a conserved dileucine motif at Leu^{309}. (De)activation of TNFα-mediated phospho-signaling cascades may unmask lysosomal targeting motifs in ZnT2 to target it to lysosomes. For example, TNFα stimulates the phosphorylation of a serine residue (Ser^{307}) in insulin receptor substrate-1 (IRS-1), which prevents its interaction with the insulin receptor and inhibits insulin signaling[44,45]. Alternatively, TNFα activates the serine/threonine phosphatase PP2A[46], which maintains Akt in its inactive dephosphorylated state and induces insulin resistance[47]. Bioinformatic analysis of ZnT2 notes several potential phosphorylation sites in proximity to both dileucine motifs. One likely phospho-signaling candidate is Ser^{296}, which is just upstream of the dileucine motif in the C-terminus of ZnT2 ($D^{292}LLLS^{296}$). Further studies are required to understand the underlying mechanism(s) that regulate the trafficking of ZnT2 to lysosomes in response to TNFα.

PCD during the second phase of involution (>48 h) is thought to be mediated by mitochondrial-mediated apoptosis[3–5]. An emerging body of evidence supports a central role for mitochondrial Zn levels in regulating apoptosis. Zn treatment in HepG-2 cells leads to Zn accumulation in mitochondria and activates p53 and its dependent genes including PUMA and Bax, contributing to a loss of mitochondrial membrane potential and activation of apoptosis[48]. Zn accumulation in mitochondria is also associated with mitochondrial depolarization, dysfunction, and cell death following neuronal ischemia[17]. Jiang et al. demonstrated that Zn induces the opening of the permeability transition pore, depolarizing the mitochondrial membrane, and activating the release of cytochrome *c* and other pro-apoptotic proteins resulting in PCD[49]. We have previously shown that ZnT2-mediated Zn accumulation in mitochondria decreases ATP production and activates apoptosis in cultured MECs[20]. Both of these biological adaptations are required to suppress the secretory phenotype of the lactating mammary gland during involution. Our studies herein implicate ZnT2-mediated mitochondrial Zn accumulation and apoptotic cell death in MECs after the initial phase of LCD during involution. However, our data do not support a role for TNFα in the process of ZnT2-mediated mitochondrial Zn accumulation. How ZnT2 is redirected away from mitochondria is not yet understood. We previously found that ZnT2 contains a motif in the N-terminus[51] HHCH[54] that is important for targeting ZnT2 for incorporation into mitochondria or the endoplasmic reticulum[20]. This motif is reminiscent of a Zn binding domain, thus we speculate that TNFα may alter Zn availability or Zn binding to this domain and redirect ZnT2 away from mitochondria and towards incorporation into the endoplasmic reticulum/vesicular system during the initial phase of mammary gland involution. However, other factors that initiate the mitochondrial-mediated pathway of apoptosis may stimulate the incorporation of ZnT2 into mitochondria as genes involved in intrinsic, mitochondrial-mediated apoptosis are activated in the later stages (i.e. > 24–48 h)[1,7,50]. Further studies are required to understand how ZnT2 is retargeted in response to regulatory stimuli.

Taken together, our studies indicate that ZnT2-mediated Zn accumulation into lysosomes and mitochondria is critical for PCD and sufficient mammary gland involution. We also provide evidence that TNFα regulates LCD of MECs through the redistribution of ZnT2-mediated Zn transport. This observation may have important implications for women with chronic inflammatory conditions of the breast that result in lactation failure, such as mastitis and obesity[51]. Moreover, inadequate PCD of MECs during involution promotes breast tumorigenesis[27]. Therefore, understanding the integration of regulatory cues and Zn metabolism may be critical to improving our

current understanding of normal mammary gland function as well as breast disease.

Methods

Mice and tissue collection. This study was approved by the IACUC Committee at The Pennsylvania State University, which is accredited by the American Association for the Accreditation of Laboratory Animal Care. All studies were conducted according to the Animal Welfare Act and Public Health Service Policy. C57BL/6 mice were obtained commercially (Charles River; Wilmington, MA, USA). Animals were maintained in a controlled environment, under consistent humidity and a 12-h light/dark cycle. All animals were fed commercially available rodent chow and had access to food and water ad libitum. For all studies, mice were euthanized by CO_2 asphyxiation and inguinal mammary glands were removed and either snap frozen on dry ice and stored at −80°C until analysis or fixed in phosphate-buffered paraformaldehyde (4%) until analysis.

Involuting mice. 12-week-old nulliparous C57BL/6 ($n = 5$) and lactating ($n = 10$) female mice were obtained commercially and housed individually. Offspring of lactating mice were culled to 8 pups/dam on lactation day 1. On lactation day 5, offspring were removed for 24 h or 48 h from a cohort of lactating mice ($n = 5$ dams) to initiate involution and then euthanized. To synchronize re-filling of mammary glands with milk, offspring were removed for 1 h, replaced for 30 min to suckle, and then removed for 3 h prior to euthanasia.

Adenoviral expression of ZnT2 in mice. AdZnT2-HA and AdLacZ vectors were generated and validated as described below. To over-express ZnT2 in the mammary glands, pregnant mice (gestation day 17) were anesthetized by isoflurane inhalation and a pulled-glass pipet containing a solution of 10^8 pfu/mL PBS and either AdZnT2-HA or AdLacZ (~50 μL) was gently inserted into the primary duct using a dissecting microscope. The mammary glands were gently infused with either AdZnT2 (mammary glands 4 and 5, $n = 9$) or AdLacZ (mammary glands 9 and 10, $n = 9$). Mice were allowed to deliver naturally and nurse their offspring for 2–3 d.

TNFα-injected mice. C57BL/6 mice were bred and litters were maintained at 6 pups/dam. TNFα (R&D Systems; Minneapolis, MN, USA) was injected into mammary glands of lactating mice as described previously[8]. Briefly, on lactation day 5, mice were anesthetized by isoflurane inhalation and TNFα (1 μg solubilized in 50 μL saline) or saline was gently injected into the mammary fat pad of gland 4 and 9, respectively using a 25-gauge needle. Pups were returned to dams for 24 h and allowed to continue nursing. Nursing was confirmed visually. Dams were euthanized and inguinal mammary glands were collected 24 h post TNFα injection.

Recombinant AdZnT2-HA and AdLacZ adenoviral vectors. The replication defective adenovirus vector AdZnT2-HA was generated using the Gateway platform[52]. A recombinant entry vector was constructed (pCR8/GW/TOPO; Invitrogen; Grand Island, NY, USA) containing a C-terminal tandem hemagglutinin (HA) tagged ZnT2 gene by PCR amplification. To generate the recombinant adenoviral DNA plasmid containing ZnT2 gene, an LR recombination reaction between the recombinant entry vector containing ZnT2-HA gene and the adenoviral destination vector (pAd/CMV/V5-DEST; Invitrogen) was performed using LR Clonase (Invitrogen) for catalysis. A recombinant adenovirus expressing β-galactosidase (pAd/CMV/V5-GW/*lacZ*; Invitrogen) was prepared according to manufacturer's instructions and used as a control vector (AdLacZ). The orientation and fidelity of the inserts were confirmed by directed sequencing (The Pennsylvania State University, Nucleic Acid Facility). Following digestion of recombinant adenoviral plasmid DNA with *Pac* I, primary viral stocks were prepared by infecting the AdZnT2-HA or AdLacZ vectors into host HEK 293A cells (Invitrogen). Adenovirus stocks were further amplified and purified by a cesium chloride gradient, titrated by plaque assay, and stored at −80°C until use.

Subcellular fractionation. Mammary glands from lactating and involuting mice were homogenized on ice in homogenization buffer (20 mM HEPES, pH 7.4, 1 mM EDTA, 250 mM sucrose, and protease inhibitors), centrifuged at 2,000 × *g* for 5 min, and crude membrane proteins and mitochondria were isolated as described previously[20,53]. Mitochondria-enriched fractions were isolated by centrifugation at 12,000 × *g* for 12 min. Lysosome-enriched fractions were isolated by pelleting the supernatant taken from the mitochondrial fraction at 25,000 × *g* for 30 min. The supernatant from the lysosome-enriched fractions was centrifuged at 100,000 × *g* for 30 min to pellet the endoplasmic reticulum/Golgi apparatus-enriched fractions. The supernatant was collected as the cytosolic fraction.

Immunohistochemistry. Mammary glands were fixed, embedded in paraffin and sectioned (5 μm) as described previously[54]. Tissues sections were permeabilized with 0.2% Triton X-100 (Sigma-Aldrich; St. Louis, MO, USA) in PBS (pH 7.4) for 45 min or ice-cold 100% methanol for 10 min and blocked in 10% goat serum, 0.05% Tween-20 (Sigma-Aldrich). Primary antibodies were pStat3 (1 : 400; Cell Signaling; Beverly, MA, USA) and cathepsin B (1 : 50; Santa Cruz; Dallas, TX, USA) and secondary antibodies were Alexa Fluor 488 or 568 goat anti-rabbit IgG (1 : 1,000; Invitrogen). HA and Lamp1 were detected with mouse anti-HA IgG, Alexa Fluor 488 conjugate (1 : 1,000; Invitrogen) and Alexa Fluor 647 anti-mouse Lamp1 (1 μg/mL; BioLegend, San Diego, CA, USA). Nuclei were stained with 4′, 6-Diamidino-2-Phenylindole, dilactate (DAPI; 1 : 20; Invitrogen). For cultured cells, coverslips were fixed in 4% w/v phosphate buffered-paraformaldehyde (pH 7.4) for 10 min and permeabilized with 0.2% Triton X-100 (Sigma-Aldrich) in PBS for 10 min. The coverslips were then blocked with 5% goat serum in PBS for 20 min. Slides were mounted in ProLong Gold (Invitrogen) and imaged on an Olympus FV1000 (Olympus; Center Valley, PA, USA) as described below or by light microscopy (Leica DM IL LED, Leica Microsystems GmbH; Wetzlar, Germany) and images were captured using Leica Application Suite (version 3.6.0).

Hematoylin and eosin staining. Morphology was examined with hematoxylin and eosin (H&E) staining as described previously[54].

TUNEL staining. The percentage of TUNEL-positive cells was quantified using the TACS XL TUNEL Basic Kit (Trevigen, Inc.; Gaithersburg, MD, USA). The number of TUNEL-positive cells in 3, 10 × fields of view per section were counted and presented as a percentage (mean number of positive-stained cells/total × 100).

Staining of mammary gland whole mounts. Inguinal mammary glands ($n = 3$–5/group) were carefully dissected, spread on a glass slide, and fixed overnight in Carnoy's solution (ethanol/glacial acetic acid, 3 : 1). Samples were rehydrated (70% ethanol for 30 min, 50% ethanol for 30 min, 30% ethanol for 20 min, 10% ethanol for 20 min, and distilled water for 5 min). Staining was performed overnight with carmine alum (0.2% carmine dye and 0.5% aluminum potassium sulfate) followed by dehydration the following day (70% ethanol for 30 min, 90% ethanol for 30 min, and 100% for 30 min). Mammary glands were cleared with xylene overnight. Sections were examined on an Olympus BX60 wide-field microscope (Olympus).

Cathepsin B activity. Cathepsin B activity was measured using the Cathepsin B Activity Fluorometric Assay Kit (BioVision; Milpitas, CA, USA). Lysosomal and cytosolic fractions were isolated as described above. Lysosomal membranes were disrupted by three freeze thaw cycles and protein concentration of the fractions was determined by Bradford assay (Bio-Rad; Hercules, CA, USA). Equal amounts of sample and reaction buffer (50 μL) were added to a 96-well plate and incubated with 2 μL of cathepsin B substrate sequence RR labeled with amino-4-trifluoromethyl coumarin (Ac-RR-AFC) for 2 h at 37°C. A sample with cathepsin B inhibitor was run in parallel. Fluorescence (excitation 400 nm/emission 505 nm) was measured on a FLUOstar OPTIMA plate reader (BMG Labtech; Ortenberg, Germany) spectrofluorometer with FLUOstar OPTIMA software version 1.32R2. Fold-increase in cathepsin B activity was determined by comparing the relative fluorescence units/mg protein after subtracting the sample with the inhibitor.

Cell culture. Mouse MECs (HC11) were a gift from Dr. Jeffery Rosen (Baylor College of Medicine; Houston, TX, USA) and used with permission of Dr. Bernd Groner (Institute for Biomedical Research; Frankfurt, Germany). Cells were maintained in "growth medium" (RPMI 1640 supplemented with 10% fetal bovine serum, 5 μg/mL insulin, 10 ng/mL epidermal growth factor, and gentamycin). For TNFα experiments, cells were pre-treated with $ZnSO_4$ (10 μM) for 5 h in growth medium followed by ± TNFα (15 ng/mL) for 24 h in serum-free medium at 37°C.

Small interfering RNA (siRNA)-mediated gene attenuation. Cells were seeded in 6-well plates in antibiotic-free medium overnight. At 50% confluency cells were transfected with 100 pmol of ZnT2-specific (sense, 5′-CCAUCUGCCUGGUG-UUCAU-3′; antisense, 5′-AUGAACACCAGGCAGAUGG-3′; Sigma-Aldrich) or mismatched control (sense, 5′-CCGCGUCCUUCCUUAUGUAGGAAUU-3′; antisense, 5′-AAUUCCUACAUAAGGAAGGACGCGG-3′; Invitrogen) siRNA using Lipofectamine 2000 (Invitrogen) at an oligonucleotide/transfection reagent ratio of 25 : 1 in OptiMEM (Invitrogen) as previously described[55]. OptiMEM was replaced 6 h later with antibiotic-free growth medium and cells were cultured overnight prior to experiments.

Cell viability. Cells were washed twice with PBS, trypsinized for 5 min at 37°C, and collected in an equal volume of medium. Cells were pelleted at 1,000 × *g* for 10 min. Cell pellets were resuspended in 100 μL growth medium, mixed with trypan blue (1 : 5; Sigma-Aldrich), and the number of viable cells was counted. Data represent cell number as a percentage of untreated control ± SD.

Zn fluorometry. FluoZin-3-AM and RhodZin-3-AM are Zn-specific (K_d 15 nM and 65 nM) fluoroionophores used to verify changes in labile Zn pools[28] and mitochondrial Zn pools[29], respectively. Cells were rinsed with 1 × PBS, pH 7.4, and loaded with either FluoZin-3-AM (2 μM; Invitrogen) or RhodZin-3-AM (1 μM; Invitrogen) for 1 h as recommended by the manufacturer in Opti-MEM containing 0.2% pluoronic acid 127. Cells were treated with Zn (1 μM) overnight as a positive control. Cells were rinsed two times with PBS, pH 7.4, and incubated for 30 min at 25°C with constant shaking. Fluorescence of FluoZin-3-AM (emission 485 nm/excitation 520 nm) and RhodZin-3-AM (emission 560 nm/excitation 595 nm) was measured at 25°C using FLUOstar OPTIMA plate reader. Cellular protein concentration was determined by Bradford assay and fluorescence measurements were normalized to total protein concentration.

^{65}Zn assay. To determine whether TNFα accumulated Zn in MECs *in vitro*, we measured Zn secretion and uptake using ^{65}Zn. HC11 cells cultured to ~70% confluency in 24-well dishes were loaded with 0.1 μCi ^{65}Zn (PerkinElmer; Waltham,

MA, USA) in serum-free medium containing 0.1 μM $ZnSO_4$ and incubated at 37°C for 3 h. Cells were washed with PBS containing 1 mM EDTA to remove any exofacially-bound ^{65}Zn and were then stimulated with TNFα or left untreated as described above. Conditioned media was removed, cells were collected, and radioactivity was quantified using a γ-scintillation counter (Packard Minaxi-γ; Packard Instrument; Meriden, CT, USA). Values represent mean pmol Zn/μg protein.

Confocal microscopy. *Subcellular localization of ZnT2.* Cells were fixed in 4% w/v phosphate buffered-paraformaldehyde (pH 7.4) for 10 min, washed in PBS, and permeabilized with 0.2% Triton X-100 (Sigma-Aldrich) in PBS for 10 min. Coverslips were then blocked with 5% goat serum/1% bovine serum albumin in PBS for 20 min followed by incubation with affinity purified rabbit anti-ZnT2 antibody[18] (1 μg/mL) or anti-HA antibody (1 μg/mL; Sigma-Aldrich) for 1 h. Following washing with PBS, antibody was detected with Alexa 488-conjugated anti-rabbit IgG (1 μg/mL; Invitrogen) for 45 min. Coverslips were washed, mounted in ProLong Gold (Invitrogen), and sealed with nail polish. Subcellular colocalization markers were as follows: mitochondria (mouse anti-COX IV antibody, 1 μg/mL; Invitrogen), lysosomes (mouse anti-Lamp1 antibody, 1 μg/mL; Abcam; Cambridge, MA, USA). Colocalization antibodies were detected with Alexa 568-conjugated anti mouse IgG (Invitrogen).

Lysosomal Zn pools. Cells were incubated with LysoTracker Red (75 nM; Invitrogen) at 37°C for 1 h, rinsed with PBS, and incubated with FluoZin-3-AM (100 μM; Invitrogen) at 37°C for 1 h as described previously[21]. Following incubation, cells were rinsed twice with PBS and washed in PBS for 30 min at room temperature with constant shaking. To assess lysosomal swelling, cells were incubated with LysoTracker Green (75 nM; Invitrogen) at 37°C for 1 h, rinsed twice with PBS, and washed in PBS for 30 min at room temperature with constant shaking and imaged as described below.

Imaging. Fixed and live cell imaging was performed using an Olympus FV1000 with PlanApo 60 × or 100 × oil lens. Digital images were captured sequentially (FV10-ASW version 4.5) to eliminate potential interferences between fluorochromes; images were saved as tif files to maintain image quality. Pearson's correlation coefficients were determined by correlation analysis using Olympus FluoView Viewer. Values [−1 (no overlap of pixels) and +1 (100% overlap)] represent the mean ± SD of at least 5 fields of view from two independent experiments.

Immunoblotting. Crude membrane proteins, mitochondria, and lysosome-enriched fractions from mouse mammary gland or HC11 cells were isolated as described above and ZnT2 was detected by immunoblotting[20,53]. The protein concentration of the fractions was determined using the Bradford assay. ZnT2 antibody was detected with horseradish peroxidase-conjugated IgG and visualized by enhanced chemiluminescence (SuperSignal Femto, Pierce; Rockford, IL, USA) following exposure to autoradiography film or using IRDyes (LiCor; Lincoln, NE, USA) and imaged using an Odyssey infrared imaging system (LiCor). Ratios of signal intensities are reported under the blot.

Zn Analysis. Milk within the mammary gland was voided prior to digestion to eliminate the contribution of milk to mammary gland Zn concentration by submerging the mammary glands into an oxytocin-PBS solution (1 IU; The Pennsylvania State University Animal Resource Program, University Park, PA, USA) for 30 min. Tissue was blotted dry and samples were digested in Ultrex II Nitric Acid (VWR; West Chester, PA, USA) in mineral-free polypropylene vials at room temperature. Zn concentration was analyzed by atomic absorption spectroscopy as described previously[56] using an Atomic Absorption Analyst 400 (PerkinElmer) and data were analyzed using WinLab32 software.

Acid phosphatase assay. Acid phosphatase activity was measured using the Acid Phosphatase Kit, according to the manufacturer's instructions (Sigma-Aldrich). In brief, the reaction mixture [sample + substrate solution (4-nitrophenyl phosphate in 0.09 M citrate buffer, pH 4.8)] was incubated for 30 min at 37°C using a horizontal shaker. The reaction was terminated by the addition of 0.5 N NaOH and absorption was measured at 405 nm. The activity was expressed as units/mL/unit of protein.

Statistical analysis. All experiments were performed in triplicate and repeated at least three times unless indicated otherwise. Western blots were repeated three times. Results are presented as mean ± standard deviation (SD). Statistical comparisons were performed using Student's *t*-test or one-way ANOVA where appropriate (Graph Pad Prism; Berkeley, CA, USA) and statistical difference was demonstrated at $P < 0.05$.

1. Kreuzaler, P. A. *et al.* Stat3 controls lysosomal-mediated cell death in vivo. *Nat Cell Biol* **13**, 303–309 (2011).
2. Arnandis, T. *et al.* Calpains mediate epithelial-cell death during mammary gland involution: mitochondria and lysosomal destabilization. *Cell Death Differ* **19**, 1536–1548 (2012).
3. Stein, T., Salomonis, N. & Gusterson, B. A. Mammary gland involution as a multi-step process. *J Mammary Gland Biol Neoplasia* **12**, 25–35 (2007).
4. Baxter, F. O., Neoh, K. & Tevendale, M. C. The beginning of the end: death signaling in early involution. *J Mammary Gland Biol Neoplasia* **12**, 3–13 (2007).
5. Watson, C. J. Involution: apoptosis and tissue remodelling that convert the mammary gland from milk factory to a quiescent organ. *Breast Cancer Res* **8**, 203 (2006).
6. Foghsgaard, L. *et al.* Cathepsin B acts as a dominant execution protease in tumor cell apoptosis induced by tumor necrosis factor. *J Cell Biol* **153**, 999–1010 (2001).
7. Clarkson, R. W., Wayland, M. T., Lee, J., Freeman, T. & Watson, C. J. Gene expression profiling of mammary gland development reveals putative roles for death receptors and immune mediators in post-lactational regression. *Breast Cancer Res* **6**, R92–109 (2004).
8. Levy, C. S. *et al.* Tumor necrosis factor alpha induces LIF expression through ERK1/2 activation in mammary epithelial cells. *J Cell Biochem* **110**, 857–865 (2010).
9. Kritikou, E. A. *et al.* A dual, non-redundant, role for LIF as a regulator of development and STAT3-mediated cell death in mammary gland. *Development* **130**, 3459–3468 (2003).
10. Boya, P. & Kroemer, G. Lysosomal membrane permeabilization in cell death. *Oncogene* **27**, 6434–6451 (2008).
11. Ono, K., Kim, S. O. & Han, J. Susceptibility of lysosomes to rupture is a determinant for plasma membrane disruption in tumor necrosis factor alpha-induced cell death. *Mol Cell Biol* **23**, 665–676 (2003).
12. Hwang, J. J., Lee, S. J., Kim, T. Y., Cho, J. H. & Koh, J. Y. Zinc and 4-hydroxy-2-nonenal mediate lysosomal membrane permeabilization induced by H2O2 in cultured hippocampal neurons. *J Neurosci* **28**, 3114–3122 (2008).
13. Lee, S. J., Cho, K. S. & Koh, J. Y. Oxidative injury triggers autophagy in astrocytes: the role of endogenous zinc. *Glia* **57**, 1351–1361 (2009).
14. Hwang, J. J. *et al.* Zinc(II) ion mediates tamoxifen-induced autophagy and cell death in MCF-7 breast cancer cell line. *Biometals* **23**, 997–1013 (2010).
15. Sunderman, F. W. The influence of zinc on apoptosis. *Ann Clin Lab Sci* **25**, 134–142 (1995).
16. Feng, P. *et al.* Zinc induces mitochondria apoptogenesis in prostate cells. *Mol Urol* **4**, 31–36 (2000).
17. Medvedeva, Y. V., Lin, B., Shuttleworth, C. W. & Weiss, J. H. Intracellular Zn2+ accumulation contributes to synaptic failure, mitochondrial depolarization, and cell death in an acute slice oxygen-glucose deprivation model of ischemia. *J Neurosci* **29**, 1105–1114 (2009).
18. Lopez, V. & Kelleher, S. L. Zinc transporter-2 (ZnT2) variants are localized to distinct subcellular compartments and functionally transport zinc. *Biochem J* **422**, 43–52 (2009).
19. Iguchi, K. *et al.* High-level expression of zinc transporter-2 in the rat lateral and dorsal prostate. *J Androl* **23**, 819–824 (2002).
20. Seo, Y. A., Lopez, V. & Kelleher, S. L. A histidine-rich motif mediates mitochondrial localization of ZnT2 to modulate mitochondrial function. *Am J Physiol Cell Physiol* **300**, C1479–1489 (2011).
21. McCormick, N., Velasquez, V., Finney, L., Vogt, S. & Kelleher, S. L. X-ray fluorescence microscopy reveals accumulation and secretion of discrete intracellular zinc pools in the lactating mouse mammary gland. *PLoS One* **5**, e11078 (2010).
22. Reinhardt, T. A. & Lippolis, J. D. Mammary gland involution is associated with rapid down regulation of major mammary Ca2+-ATPases. *Biochem Biophys Res Commun* **378**, 99–102 (2009).
23. Fujimoto, S. *et al.* Zinc-ion-dependent acid phosphatase exhibits magnesium-ion-dependent myo-inositol-1-phosphatase activity. *Biol Pharm Bull* **19**, 882–885 (1996).
24. Helminen, H. J. & Ericsson, J. L. Quantitation of lysosomal enzyme changes during enforced mammary gland involution. *Exp Cell Res* **60**, 419–426 (1970).
25. Russell, T. D. *et al.* Transduction of the mammary epithelium with adenovirus vectors in vivo. *J Virol* **77**, 5801–5809 (2003).
26. Nguyen, D.-A., Beeman, N., Lewis, M., Schaack, J. & Neville, M. C. *Intraductal Injection into the Mouse Mammary Gland.* (Kluwer Academic/Plenum Publishers, New York, NY, Methods in mammary gland biology and breast cancer research; 2000).
27. Radisky, D. C. & Hartmann, L. C. Mammary involution and breast cancer risk: transgenic models and clinical studies. *J Mammary Gland Biol Neoplasia* **14**, 181–191 (2009).
28. Muylle, F. A., Adriaensen, D., De Coen, W., Timmermans, J. P. & Blust, R. Tracing of labile zinc in live fish hepatocytes using FluoZin-3. *Biometals* **19**, 437–450 (2006).
29. Sensi, S. L., Ton-That, D., Weiss, J. H., Rothe, A. & Gee, K. R. A new mitochondrial fluorescent zinc sensor. *Cell Calcium* **34**, 281–284 (2003).
30. Teplova, I. *et al.* ATG proteins mediate efferocytosis and suppress inflammation in mammary involution. *Autophagy* **9**, 459–475 (2013).
31. Helminen, H. J., Ericsson, J. L. & Niemi, M. Lysosomal changes during castration-induced prostatic involution in the rat. *Acta Pathol Microbiol Scand A* **78**, 493–494 (1970).
32. Schissel, S. L., Keesler, G. A., Schuchman, E. H., Williams, K. J. & Tabas, I. The cellular trafficking and zinc dependence of secretory and lysosomal sphingomyelinase, two products of the acid sphingomyelinase gene. *J Biol Chem* **273**, 18250–18259 (1998).
33. Ohana, E. *et al.* Identification of the Zn2+ binding site and mode of operation of a mammalian Zn2+ transporter. *J Biol Chem* **284**, 17677–17686 (2009).

34. Kobayashi, T. *et al.* Late endosomal membranes rich in lysobisphosphatidic acid regulate cholesterol transport. *Nat Cell Biol* **1**, 113–118 (1999).
35. Bucci, C., Thomsen, P., Nicoziani, P., McCarthy, J. & van Deurs, B. Rab7: a key to lysosome biogenesis. *Mol Biol Cell* **11**, 467–480 (2000).
36. Lynch, C. J., Patson, B. J., Goodman, S. A., Trapolsi, D. & Kimball, S. R. Zinc stimulates the activity of the insulin- and nutrient-regulated protein kinase mTOR. *Am J Physiol Endocrinol Metab* **281**, E25–34 (2001).
37. Settembre, C. *et al.* TFEB links autophagy to lysosomal biogenesis. *Science* **332**, 1429–1433 (2011).
38. Sardiello, M. *et al.* A gene network regulating lysosomal biogenesis and function. *Science* **325**, 473–477 (2009).
39. McCormick, N. H. & Kelleher, S. L. ZnT4 provides zinc to zinc-dependent proteins in the trans-Golgi network critical for cell function and Zn export in mammary epithelial cells. *Am J Physiol Cell Physiol* **303**, C291–297 (2012).
40. Salazar, G., Falcon-Perez, J. M., Harrison, R. & Faundez, V. SLC30A3 (ZnT3) oligomerization by dityrosine bonds regulates its subcellular localization and metal transport capacity. *PLoS One* **4**, e5896 (2009).
41. Braulke, T. & Bonifacino, J. S. Sorting of lysosomal proteins. *Biochim Biophys Acta* **1793**, 605–614 (2009).
42. Wenzel, H. J., Cole, T. B., Born, D. E., Schwartzkroin, P. A. & Palmiter, R. D. Ultrastructural localization of zinc transporter-3 (ZnT-3) to synaptic vesicle membranes within mossy fiber boutons in the hippocampus of mouse and monkey. *Proc Natl Acad Sci U S A* **94**, 12676–12681 (1997).
43. Salazar, G. *et al.* The zinc transporter ZnT3 interacts with AP-3 and it is preferentially targeted to a distinct synaptic vesicle subpopulation. *Mol Biol Cell* **15**, 575–587 (2004).
44. Rui, L. *et al.* Insulin/IGF-1 and TNF-alpha stimulate phosphorylation of IRS-1 at inhibitory Ser307 via distinct pathways. *J Clin Invest* **107**, 181–189 (2001).
45. Aguirre, V. *et al.* Phosphorylation of Ser307 in insulin receptor substrate-1 blocks interactions with the insulin receptor and inhibits insulin action. *J Biol Chem* **277**, 1531–1537 (2002).
46. Cornell, T. T. *et al.* Ceramide-dependent PP2A regulation of TNFalpha-induced IL-8 production in respiratory epithelial cells. *Am J Physiol Lung Cell Mol Physiol* **296**, L849–856 (2009).
47. Teruel, T., Hernandez, R. & Lorenzo, M. Ceramide mediates insulin resistance by tumor necrosis factor-alpha in brown adipocytes by maintaining Akt in an inactive dephosphorylated state. *Diabetes* **50**, 2563–2571 (2001).
48. Rudolf, E. & Cervinka, M. Zinc pyrithione induces cellular stress signaling and apoptosis in Hep-2 cervical tumor cells: the role of mitochondria and lysosomes. *Biometals* **23**, 339–354 (2010).
49. Jiang, D., Sullivan, P. G., Sensi, S. L., Steward, O. & Weiss, J. H. Zn(2+) induces permeability transition pore opening and release of pro-apoptotic peptides from neuronal mitochondria. *J Biol Chem* **276**, 47524–47529 (2001).
50. Stein, T. *et al.* Involution of the mouse mammary gland is associated with an immune cascade and an acute-phase response, involving LBP, CD14 and STAT3. *Breast Cancer Res* **6**, R75–91 (2004).
51. Rasmussen, K. M. Association of maternal obesity before conception with poor lactation performance. *Annu Rev Nutr* **27**, 103–121 (2007).
52. Walhout, A. J. *et al.* GATEWAY recombinational cloning: application to the cloning of large numbers of open reading frames or ORFeomes. *Methods Enzymol* **328**, 575–592 (2000).
53. Seo, Y. A. & Kelleher, S. L. Functional analysis of two single nucleotide polymorphisms in SLC30A2 (ZnT2): implications for mammary gland function and breast disease in women. *Physiol Genomics* **42A**, 219–227 (2010).
54. Kelleher, S. L. & Lonnerdal, B. Zinc transporters in the rat mammary gland respond to marginal zinc and vitamin A intakes during lactation. *J Nutr* **132**, 3280–3285 (2002).
55. Chowanadisai, W., Lönnerdal, B. & Kelleher, S. L. Identification of a mutation in SLC30A2 (ZnT-2) in women with low milk zinc concentration that results in transient neonatal zinc deficiency. *J Biol Chem* **281**, 39699–39707 (2006).
56. Clegg, M. S., Lönnerdal, B., Hurley, L. S. & Keen, C. L. Analysis of whole blood manganese by flameless atomic absorption spectrophotometry and its use as an indicator of manganese status in animals. *Anal Biochem* **157**, 12–18 (1986).

Acknowledgments

The authors gratefully acknowledge the technical expertise of Drs. Samina Alam, Claire Berryman, Veronica Lopez, and Nicholas McCormick and Thomas Croxford, Michael Lanz, and Sooyen Lee. We would also like to acknowledge Dr. Margaret Neville for her expertise in developing the transduced mammary gland model. All confocal microscopy was done at the Cytometry Facility (Huck Institutes of the Life Sciences, The Pennsylvania State University). This work was supported by NIH 058614 to S.L.K. and Intramural Support from the Department of Surgery to D.I.S.

Author contributions

S.R.H., S.S. and S.L.K. conceived and designed the research; S.L.K and D.I.S. supported the research. Y.A.S. and S.S. generated and validated the ZnT2 adenovirus. S.R.H. conducted the experiments; S.R.H. analyzed the data; S.R.H. and S.L.K. interpreted and the data; S.R.H. wrote the manuscript with input from S.L.K. and D.I.S.

Additional information

Supplementary information accompanies this paper at http://www.nature.com/scientificreports

Competing financial interests: The authors declare no competing financial interests.

How to cite this article: Hennigar, S.R., Seo, Y.A., Sharma, S., Soybel, D.I. & Kelleher, S.L. ZnT2 is a critical mediator of lysosomal-mediated cell death during early mammary gland involution. *Sci. Rep.* **5**, 8033; DOI:10.1038/srep08033 (2015).